Scanning Microscopy

Volume 1 | Number 4 Article 46

8-28-1987

Scanning Microscopic Observations on Dental Caries

Sheila J. Jones
University College London

Alan Boyde
University College London

Scanning Microscopy, Vol. 1, No. 4, 1987 (Pages 1991-2002)
Scanning Microscopy International, Chicago (AMF O'Hare), IL 60666 USA

0891-7035/87$3.00+.00

SCANNING MICROSCOPIC OBSERVATIONS ON DENTAL CARIES

Sheila J Jones & Alan Boyde

Hard Tissue Unit, Department of Anatomy and Developmental Biology,
University College London,
Gower Street, LONDON, WC1E 6BT, England

(Received for publication May 05, 1987, and in revised form August 28, 1987)

Abstract

This paper presents findings made using special techniques of imaging and/or of specimen preparation to investigate the changes in tooth structure which occur in caries. We have studied both coronal and root caries in enamel, dentine and cementum using scanning electron and confocal scanning optical microscopy.

In preparation for backscattered electron (BSE) imaging in the SEM, teeth were stored in 70% ethanol until further dehydration in ethanol and embedding in polymethylmethacrylate (PMMA). Longitudinally cut surfaces were diamond polished and coated with carbon or silver before BSE imaging. Important changes in the distribution of densities in both enamel and dentine occurred during caries, and could be correlated with prior published studies using polarised light and microradiography to study demineralization in these tissues. However, the resolution of the BSE imaging technique is much higher than that of these previous methods.

A new method was used for demonstrating local variations in microhardness with special relevance to the changes occurring in dental caries. Sectioned surfaces were subjected to treatment with a jet of soft abrasive particles, resulting in the selective removal of carious enamel, and enhanced removal of carious dentine.

The tandem scanning reflected light microscope (TSRLM) has also been shown to be useful in characterising the spread of caries in the dental tissues. Teeth only need to be cut once, because the image is formed on looking into a bulk specimen. Fluorescent dyes can be used to study the distribution of pore volume, making use of the high resolution in depth of this confocal microscope.

KEY WORDS: Caries, enamel, dentine, cementum, backscattered electrons, microhardness, Air polishing, confocal scanning optical microscopy.

*Address for correspondence: Sheila Jones or Alan Boyde. Department of Anatomy, University College London, Gower Street, LONDON, WC1E 6BT
Phone No: (UK=44) (1) 387 7050 Ext 3319 or 3316

Introduction

The dental tissues were the first biological tissues to be studied using the scanning electron microscope, yet in spite of the fact that they are very well-suited to this type of study because of their low water content, meaning that they shrink little on preparation, the SEM has hardly been used to examine the process of change during the carious attack on dentine. Many papers have been published of SEM studies of natural and artificial enamel caries, but few of these have used the back-scattered electron imaging mode to make images which can be interpreted as demonstrating differences in density distribution.

The first SEM images of caries were made using backscattered electrons (Boyde et al. 1961, 1963). These showed that in the lesions studied the centres of enamel prisms were preferentially dissolved. They also indicated that the border of the enamel carious lesion was rather sharply demarcated: this is not the impression given in microradiographs and polarised light micrographs of enamel carious lesions. Later SEM studies of caries were concerned with the changes in gross carious lesions and, in particular, with the morphology of the products occluding dentine tubules in gross carious lesions (Lester and Boyde 1968a,b). It was shown that the material plugging dentine tubules varied in morphology from elements which could be interpreted as calcified bacteria, through plate and needle-like crystal forms, to dense plugs in which the individual crystals could not be resolved by scanning electron microscopy.

Since that time, SEM studies of both natural and artificial enamel caries have concentrated either upon attempting to visualize the route of entry of the lesion through the surface zone enamel (Brannstrom et al. 1980; Fejerskov et al. 1984; Goldberg et al. 1981; Haikel et al. 1983; Holmen et al. 1985b), or in attempting to portray the changes in crystal size and morphology and packing density in different anatomical regions within the prisms (Holmen et al. 1985a; Johnson et al. 1971; Jongebloed et al. 1975). These studies have been well-reviewed and catalogued by Shellis and Hallsworth (1987).

The purpose of the present communication is to demonstrate the features which can be seen:-

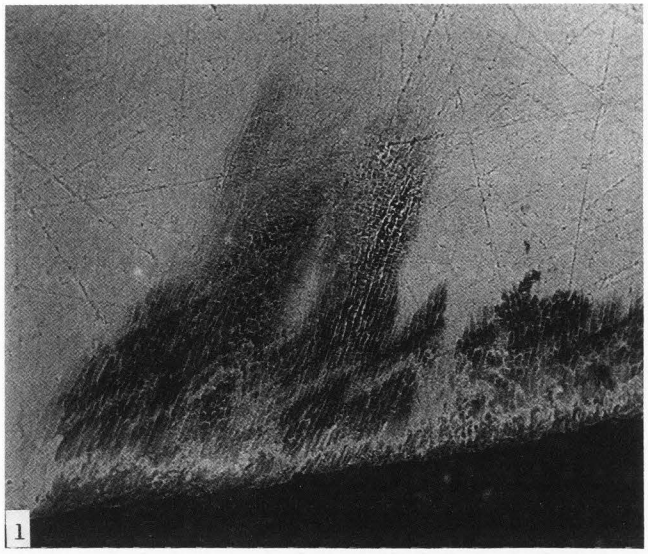
1

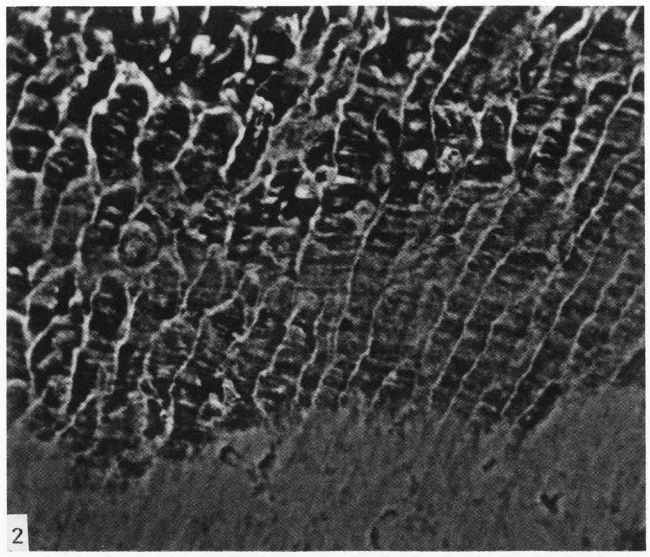
2

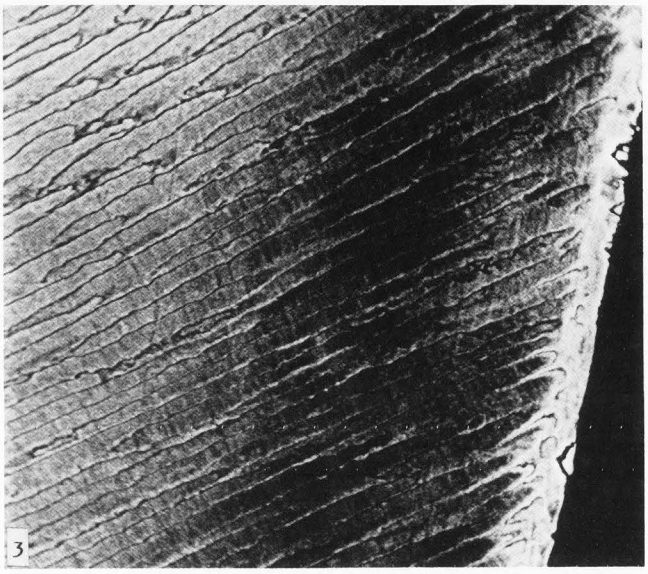
3

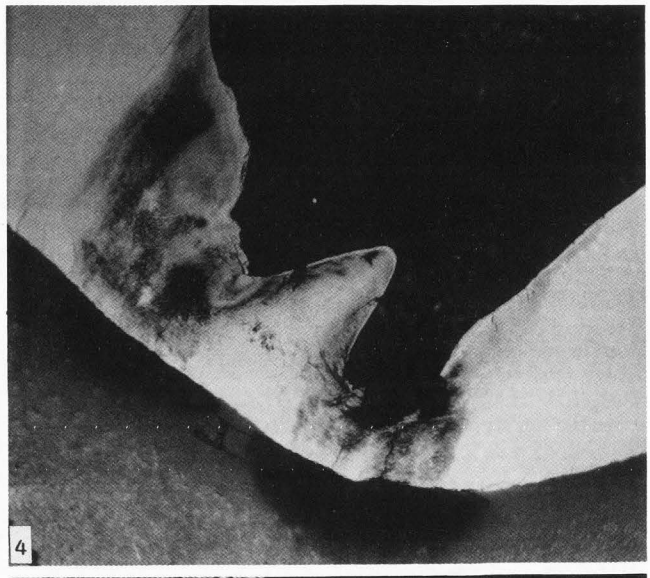
4

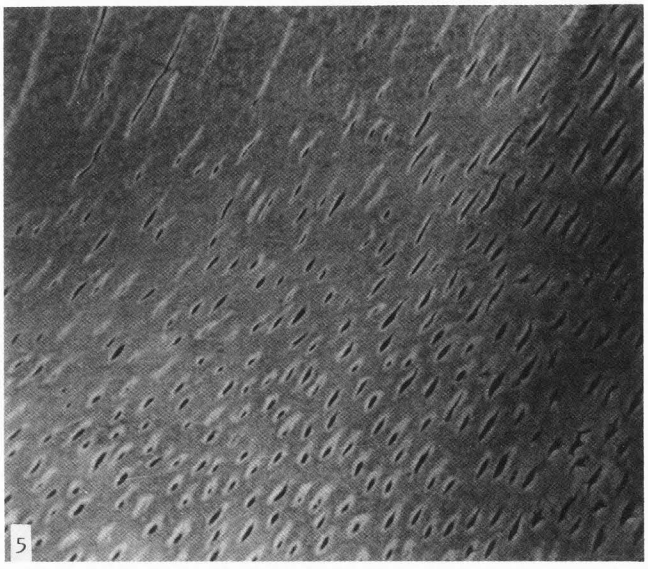
5

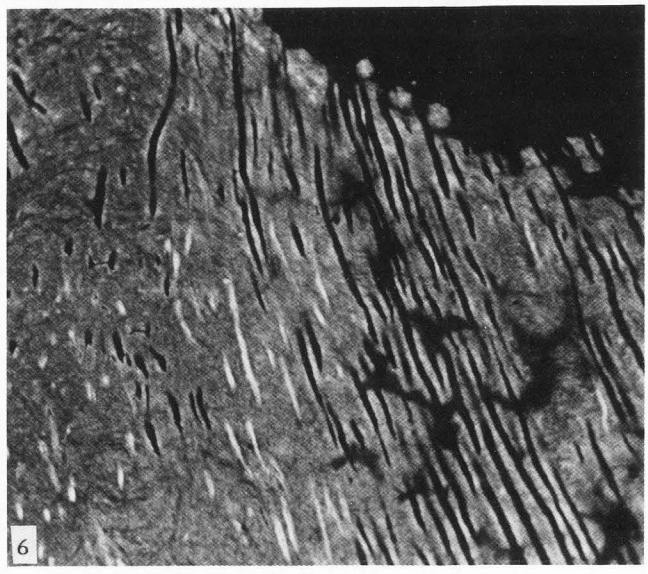
6

Figure 1. BSE SEM of longitudinal section through early approximal carious lesion in enamel. Fieldwidth = 500 μm.

Figure 2. Higher power view of the advancing border of an enamel lesion showing the prominence of the cross-striations of the enamel prisms, and the prism boundary or junction regions in the carious enamel. Fieldwidth = 100 μm.

Figure 3. A similar preparation showing subsurface demineralization, retention of normal mineralization levels in the deeper enamel (left) and a high degree of mineralization in the surface enamel (right). More detail of the shape of the carious lesion. Fieldwidth = 180 μm.

Figure 4. Low power view of longitudinal section of tooth with occlusal carious lesions which have progressed through into the underlying dentine. Fieldwidth = 2000 μm.

Figure 5. View showing the border zone of an occlusal carious lesion with occluded dentine tubules with peritubular zones flanking the lesion, and the absence of peritubular dentine in the affected tissue. Fieldwidth = 195 μm.

Figure 6. Secondary dentine formation below a carious lesion. The dentine at right shows many interglobular regions and a calcospheritic mineralization. The dentine to the left, below a sclerosed tract, shows occlusion of dentine tubules with peritubular dentine. Fieldwidth = 470 μm.

****

1) in backscattered electron imaging of coronal and root carious lesions; 2) in the process of the physiological resorption of dentine which has previously been involved in a carious lesion; 3) in secondary electron images of carious lesions prepared by a technique which demonstrates variations in the microhardness of the tissue, consequent upon the partial demineralization. 4) In addition, we demonstrate preliminary results obtained by the new technique of Tandem Scanning Reflected Light Microscopy (TSRLM), in particular the fluorescence mode, in studying the progress of the enamel and dentine carious lesions using fluorescent markers to probe the extent of increased porosity at the margin of the lesion.

Materials and Methods

Teeth extracted for a variety of clinical; reasons, including overcrowding, periodontal condition and pulpitis following caries were fixed and stored in 70% ethanol until routine preparation for conventional SEM. Aldehyde based fixatives were avoided because they may result in a partial demineralization of the tissue, and in the context of the TSRLM, aldehyde fixation induces a change in the autofluorescence of the tissues.

Preparation for atomic number contrast BSE-SEM

The samples were rigorously extracted with chloroform-methanol in a Soxhlet apparatus, substituted with freshly flash-distilled methyl methacrylate monomer, and embedded in a mixture of 5% styrene, 95% methyl methacrylate destabilised with 2,2'-azo-bis-(2-methyl-proprionitrile) (Sigma Chemical Co.) and polymerised at 30°C. The embedding and polymerisation schedules lasted for considerable periods (eg. 1 month) - the purpose of which was to ensure the thorough infiltration of all small spaces in the tissue.

Following embedment, the blocks were cut in the longitudinal direction, serially ground and polished to a 1 micron-diamond finish. They were then coated with either carbon or silver, and imaged in a Cambridge S4-10 Stereoscan SEM operated at 20 kV (e.g., Figures 1-7). A KE Electronics annular, 4 segment, solid-state, BSE detector was used with the sample at normal incidence to the electron beam. By adding the signal from all 4 detectors segments, an image was obtained representing density variations in the sample surface. By subtracting the signal from two opposing detector segments, images could be obtained demonstrating the topographic relief resulting from the polishing procedure. The latter images were necessary to check upon the validity of interpretation of the former as being due entirely to variations in density (Boyde and Jones 1983: Boyde 1984a).

Airpolishing™

To demonstrate the variations in microhardness in both enamel and dentine, unembedded teeth were cut in the longitudinal direction and the cut surface treated with an air-propelled jet of sodium bicarbonate powder, shrouded by a concentric water jet. This technique results in the removal of softened enamel and dentine and can be used to "dissect out" the carious lesion (Boyde 1984b, 1985). These samples were washed, dehydrated in ethanol and air dried from $C_2Cl_3F_3$ and imaged using either SE or BSE (Figs 8 and 9).

Tandem Scanning Reflected Light Microscopy (TSRLM)

Teeth with natural and artificial carious lesions were sectioned in the longitudinal direction and imaged in the usual reflective mode in the TSRLM (Fig. 10) (Boyde et al 1983; Petran et al 1985; Boyde 1985, 1986). Others were soaked in a solution of brilliant sulphaflavine in 50% ethanol, tetracycline in water, or alizarine red S. They were removed from this solution, the surplus removed by rapid blotting, and then covered with microscope immersion oil, prior to examination with oil immersion objectives, fluorescence objectives in the TSRLM (Fig. 11). Particular attention was paid to the morphology of the edge of the advancing lesion, and to the gross distribution of intensity of fluorescent stain incorporated within the pore volume of the carious lesion. Carious teeth were also stained using a solution of brilliant sulphaflavine in 50% ethanol prior to (the above described method of) embedding in PMMA so that a correlation could be made between TSRLM and BSE images.

Results

Normal tissues

BSE imaging of normal enamel has been described previously by Boyde (1979) and Boyde & Jones (1983). It is not possible to demonstrate the variations in the mineral content known to exist across the thickness of normal enamel (higher at the enamel dentine junction and the enamel surface than in the centre of the enamel) using low magnification BSE imaging.

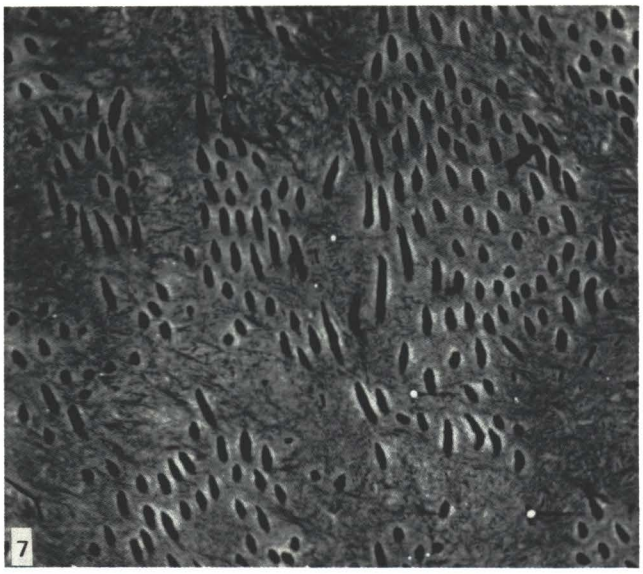
7

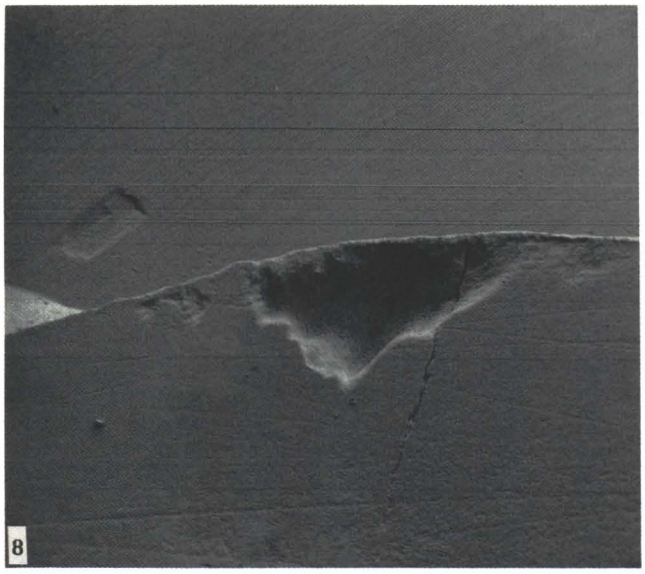
8

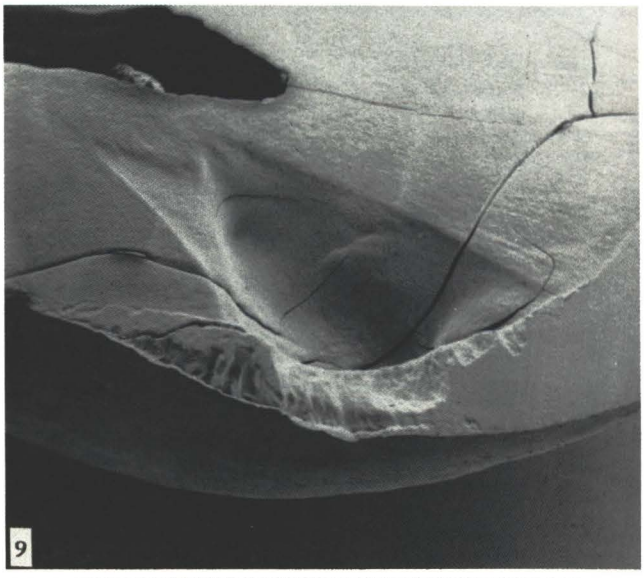
9


10


11

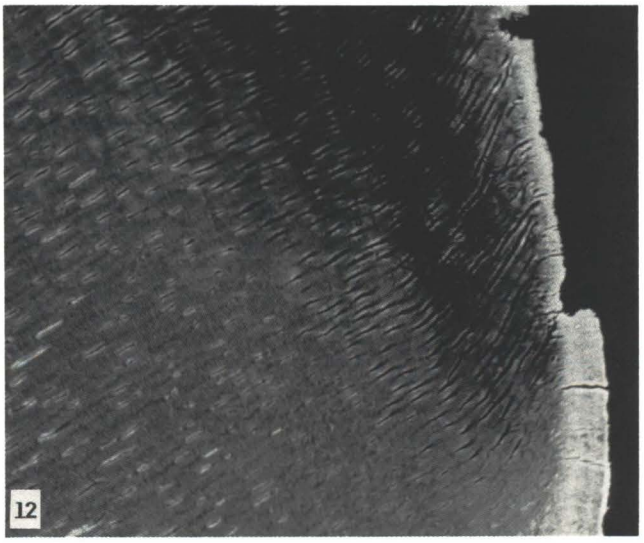
12

Figure 7. Secondary dentine formation at the pulpal aspect of a carious lesion: regions devoid of tubules are interspersed between patches where the tubules are regularly arranged. This shows as a variation in overall mineralization in lower resolution, lower magnification images. Field-width = 160 μm.

Figure 8. Low power BSE A-B (topographic) image of longitudinal section through an interproximal carious lesion which was then air-polished to remove the softened carious enamel to provide a view of the three-dimensional extent of the lesion. Fieldwidth = 2mm.

Figure 9. Similar preparation of a carious lesion which had penetrated into dentine showing the exploration of the dentine lesion as a function of its hardness. Fieldwidth = 5 mm.

Figure 10. TSRLM reflected light image of an interproximal carious lesion. Fieldwidth = 320 μm.

Figure 11. TSRLM image of an interproximal carious lesion soaked in a brilliant sulphaflavine solution and imaged by the yellow fluorescence of this material under a blue light illumination. Fieldwidth = 400 μm.

Figure 12. Root caries: low power BSE showing the cervical border of an extensive lesion in longitudinal section. Fieldwidth = 400 μm.

****

Low magnifications imply large field widths, so that different parts of the field are at different distances from different portions of the detector array which may function with different efficiencies. (This problem could be taken care of by an approach similar to the shading correction procedure used in light microscopic image analysis, but this has not, to the authors' knowledge, yet been instituted in the context of BSE image analysis in an SEM: it would require an analogous, extremely uniform standard: single crystal materials could not be used because of channeling contrast). At higher magnifications it can be taken that the detector response is uniform across the field, and single micrographs of limited fields within enamel demonstrate local variations in mineralization density; in particular those related to the incremental lines, the brown striae of Retzius, and the daily incremental lines - the cross striations of the enamel prisms. Towards the enamel dentine junction, the widened prism junction planes corresponding to the tufts, and the tubular defects of the enamel spindles and tubules can also easily be visualized.

In dentine, much structure that depends upon variations in the degree of mineralization can be detected using BSE imaging. At the coarser scale one may cite the fact that the intertubular dentine matrix mineralization level is obviously less than that of the synchronously or secondarily formed peritubular dentine phase (Fig. 5). At a higher resolution, it is possible to detect fine details in intertubular dentine mineralization levels which relate to the collagen fibril structure in this tissue. At a lower level of magnification, it is possible to see a structure which relates to the pattern of progress of mineralization in the dentine, namely, via the formation of calcospherites (zones at which, or by which, the dentine mineralization spreads ahead of the general mineralization front, and then spreads out spherically from each such centre). The centres of calcospherites can be seen to be denser than the more peripheral regions, as if the factor which initiates this new mineralization process is more effective in allowing it to occur at that local centre. This is true in both crown and root dentine. (Boyde and Jones 1983; Jones and Boyde 1984). In coronal dentine, there is a layer of slightly reduced mineralization just deep to the enamel dentine junction. In root dentine, there is a broad zone, the granular layer of Tomes, deep to the hyaline layer at the cement-dentine junction.

In cementum, the structures detected due to variations in the degree of mineralization include the Sharpey fibres. In secondary cementum deposition the centres of the Sharpey fibres frequently fail to mineralize and create linear mineralization defects which can, under certain circumstances, be confused with the dentine tubules. In cellular cementum, of course, the cementocyte lacunae are clearly defined "defects". In cementum which has undergone resorption-repair remodelling, the "cement" lines where new cement is attached to old dentine or cement are hypermineralized. The level of mineralization in acellular cementum as seen in BSE imaging is generally higher than that seen in the subjacent dentine.

TSRLM imaging of enamel clearly resolves all the conventional light microscopically visible structures, including the enamel prisms, their varicosities or cross-striations, the parazones and diazones of prisms having common orientation properties, the enamel spindles, tubules, tufts and lamellae. In dentine, the TSRLM is well-suited to studying the course and distribution of the major dentinal tubules and their side branches. In the latter respect it confirms that the distribution of side branches is richer in the root dentine than in crown dentine. In cementum, both the non-mineralized centres of Sharpey fibres and the cementocyte lacunae and canaliculi show to advantage. In many if not most human teeth, the TSRLM can be used to characterize cementum layers, through into dentine, without the need to cut the tooth, simply by looking through the intact root surface.

The enamel caries lesion

BSE imaging. No BSE studies of carious enamel have been published since the early reports by Boyde et al. (1961, 1963). In the present work we have been able to detect much finer differences in density distribution than was possible using the scintillator detectors available at that early time. It should be borne in mind, therefore, that the BSE images demonstrated in this paper may show very small differences in density distribution which could not be detected by other means of microscopy and certainly could not be detected by techniques of high resolution microradiography.

Teeth selected as having "white-spot" approximal surface carious lesions showed a distribution of reduction in density corresponding with the classical descriptions available from light microscopy and microradiography (Gottlieb et al. 1946) (Fig. 1). Thus, the basic morphology of the

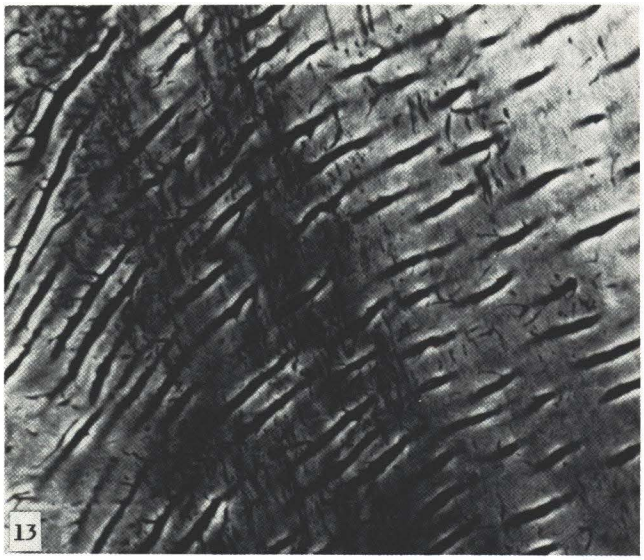
13

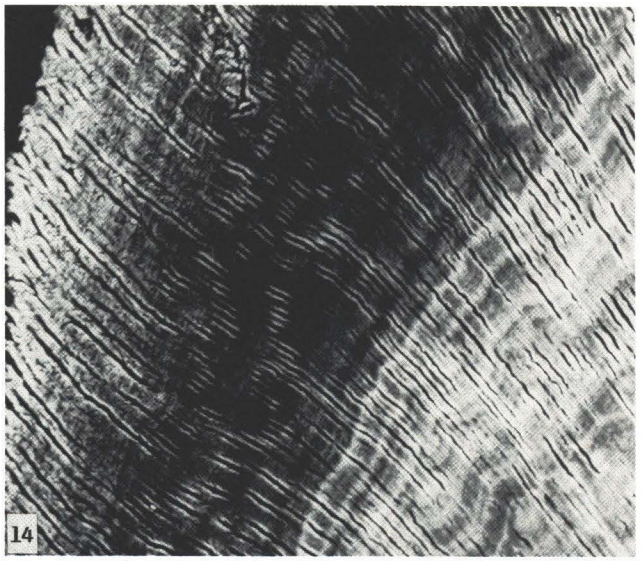
14

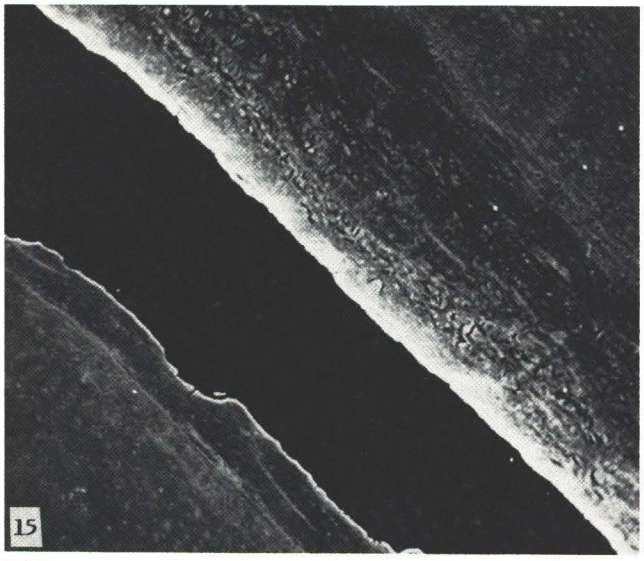
15

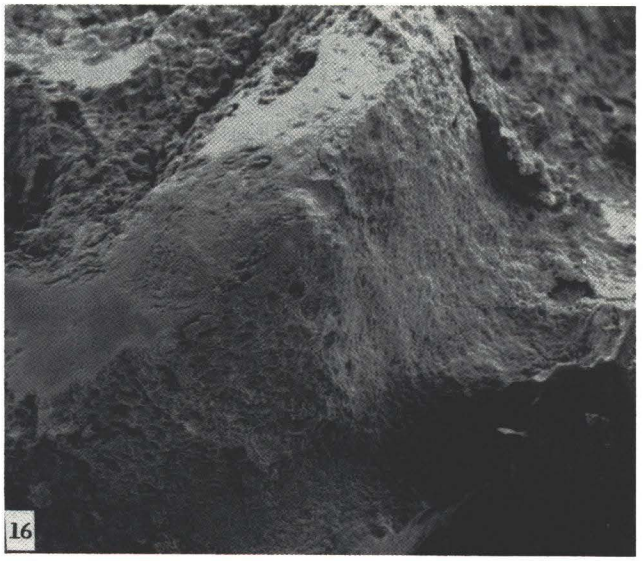
16

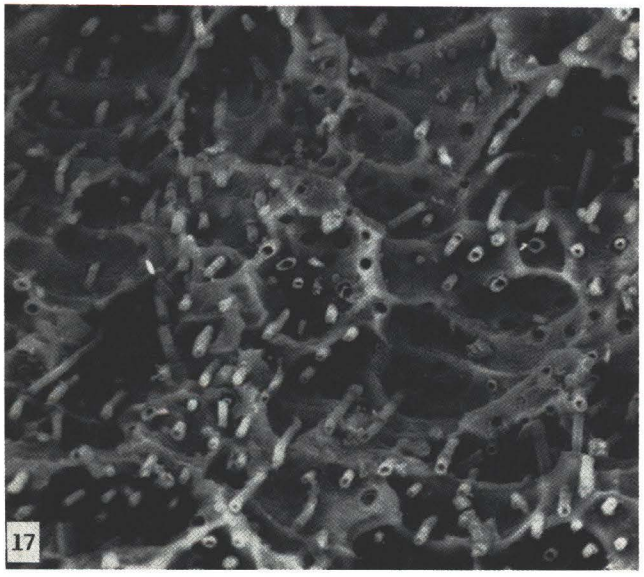
17

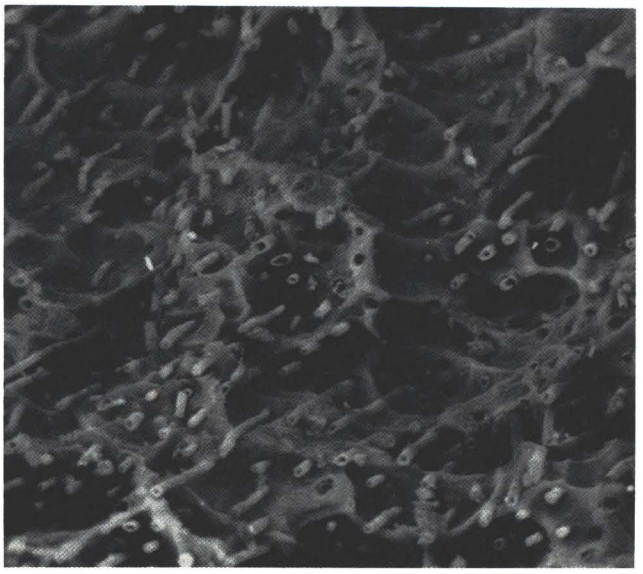

Figure 13. Root caries - higher power showing the lamination of the affected dentine parallel with the incremental direction of the collagen in the tissue and the side branches of the dentine tubules. Fieldwidth = 175 µm.

Figure 14. Carious dentine, lesion advancing to lower right, showing the prominence of the incremental growth features in the mineral phase. Fieldwidth = 400 µm.

Figure 15. Longitudinal section through a deciduous molar tooth with a coronal carious lesion, showing internal resorption of the root dentine remote both from direct involvement with the crown caries and the physiological root resorption processes. Fieldwidth = 40 µm.

Figure 16. Projection of carious dentine "rejected" by physiological resorption showing a smooth area caused by contact with the erupting permanent premolar tooth. Fieldwidth = 2 mm.

Figure 17. Carious dentine, similarly rejected by physiological osteoclastic resorption, showing projecting rods of peritubular dentine projecting from a surface showing resorption lacunae. Stereopair, tilt angle difference = 10^{o}. BSE. Fieldwidth = 90 µm.

****

lesion was, as seen in longitudinal section, triangular, with one surface of the triangle facing the just subsurface enamel, and the apex directed towards the enamel dentine junction. The finer form of the advancing edge is jagged in three dimensions, with a local variation in the rate of acid dissolution along groups of prisms (Figs. 2 & 3). The findings do not support the concept of a lateral, sideways-on attack of the carious lesion into sound enamel - as has sometimes been proposed from observations made on using lower resolution methods (Darling 1958).

The involvement of the presumed daily incremental line features, the cross-striations, of the enamel prisms in the carious process, reported by PLM and microradiography, is well demonstrated in BSE images (Figs. 2 & 3). The Hunter-Schreger bands or zones of prisms having different and contrasting common orientation properties could also be imaged to good advantage using this method, when it was demonstrated that regions where the centres of the prisms were preferentially dissolved (or retained) could easily be discriminated (Jones and Boyde 1987).

The air-polishing method for demonstrating the distribution of the enamel carious lesion has the advantage over prior methods of giving some idea of the three-dimensional distribution of the lesion (Figs. 8 & 9). However, the three-dimensional extent of the lesions that we "developed" in this way must not be interpreted too literally because the depth to which the softened carious enamel is removed depends upon the duration of the air-polishing treatment.

TSRLM. The distribution of enamel carious lesions can be studied at greater depths into the surface of the section than in the case of BSE images of polished embedded samples in the SEM using the TSRLM (Figs 10 & 11). This microscope produces an image of a very shallow depth of field seen deep to the surface of a specimen. Carious enamel contains more "space" which is more reflective than the surrounding normal enamel. Thus, the various zones in the carious lesion appear whiter and more reflective than the surrounding normal tissue as seen at a low resolution.

In specimens which had been soaked in a solution of a fluorescent stain, we were able to demonstrate gross variations in the intensity of the fluorescence image obtained at any one section level, demonstrating differences in the porosity of the tissue. At the deep, advancing surface, of the enamel lesion it was visualized as a series of deep slender pointed projections, which we interpreted as preferential opening of the prism boundary or junction regions by selective dissolution of material at the prism boundary (Fig. 11).

The dentine caries lesion

The BSE SEM image of the dentine carious lesion provides a very simple and dramatic way of illustrating the extent of advance of the lesion and the response of the tissue (Figures 5-7, 12-14). The present studies have brought the following features of the spread of the carious lesion into prominence.

First, we have noticed that, contrary to the general description available in textbook literature (stating that once the carious lesion has penetrated through enamel into dentine, it spreads parallel to the enamel dentine junction much more rapidly than in depth), we have been able to find examples of lesions in which the extent of the enamel involvement at the EDJ was either greater than, or equal to, that in the subjacent dentine. Nevertheless, there are differences in the dentine, immediately deep to the enamel dentine junction, which would explain the rapid lateral spread of the lesion in this region which is sometimes also seen. In large lesions, undermining and reverse involvement of enamel may occur: the hidden carious lesion being a recent clinical phenomenon below fluoride- rich surface enamel.

In the case of lesions which had progressed deep into the dentine, these demonstrated a rather sharp lateral border. In dentine tubules parallel to the edge of the lesion, zones of the highly mineralized peritubular dentine phase were found (Fig 5). In the tubules adjacent to these, towards the centre of the lesion, peritubular zones were removed. Further towards the centre of the lesion, there was a general reduction in density of the intertubular dentine matrix, and the formation of clefts, or holes, in the structure which we cannot exclude as being partly due to shrinkage artifact during the dehydration stages of specimen preparation. Thus, we cannot be sure that any major deficiencies in the grossly cariously involved dentine structure are not, at least partly, an artifact of specimen preparation. In this context, the present methodology is no different than the methodologies of light microscopy and polarised light microscopy, and we would make the same caveats concerning the interpretation of the defects seen in sections using other methods of microscopy. At the deep advancing surface of the dentine lesion, that is, where the process is to be interpreted as involving dentine tubules seen in transverse section, a considerable increase in the general density of the dentine could be noted at low resolution. At higher

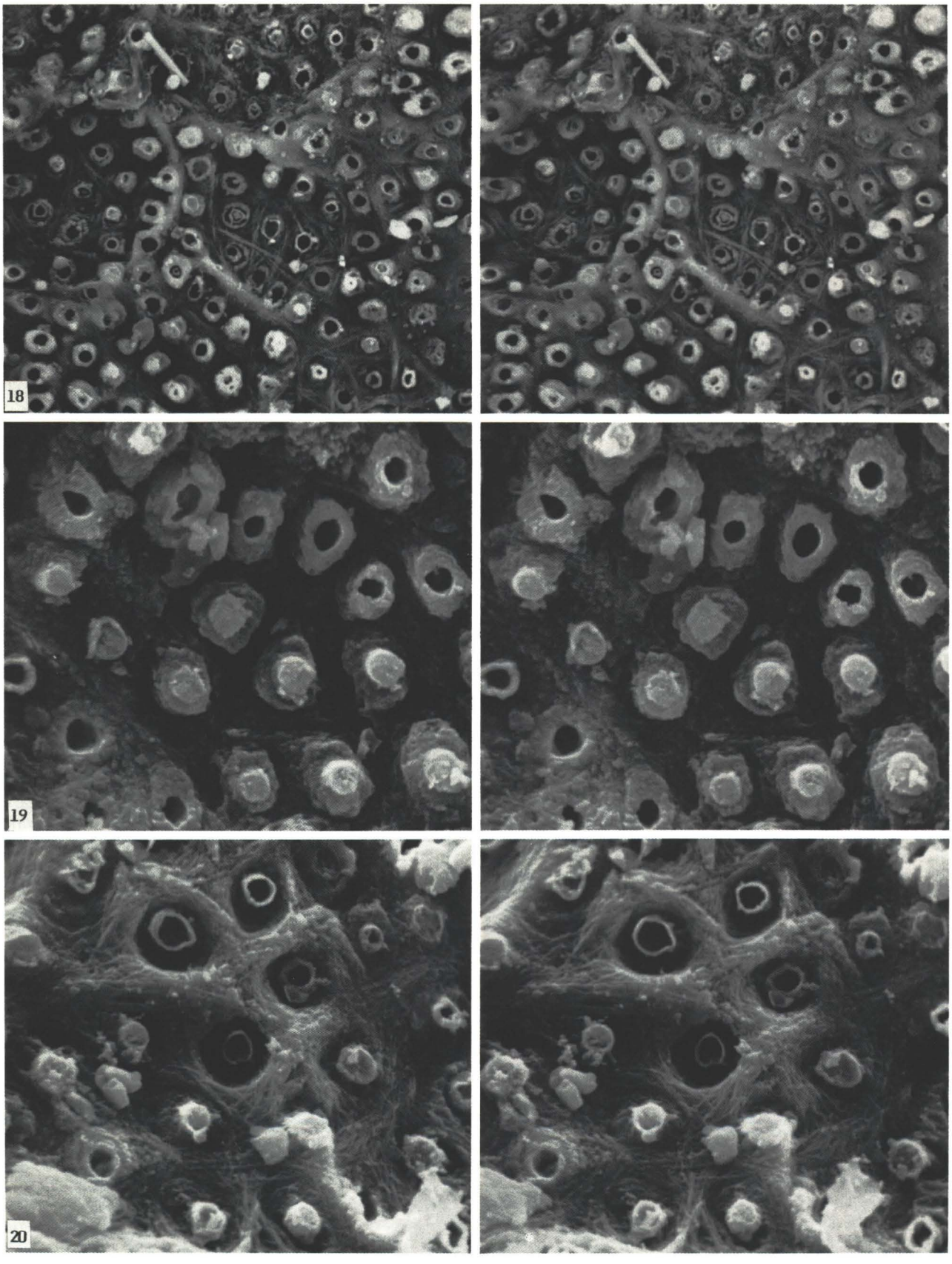
18
19
20

Figure 18. Resorption lacunae in carious dentine. At centre and at left can be seen areas in which the pattern of organisation of the original dentine matrix collagen has been exposed. Some tubules are completely occluded, some contain tubes of intratubular dentine mineralization within the peritubular dentine zone. At top right can be seen a rod of intratubular dentine which has fallen on to the surface: this is not in its original location. Stereopair, tilt angle difference = 10^{0}. BSE. Fieldwidth = 47µm.

Figure 19. Higher power view of resorbed carious dentine showing, under stereo viewing, the projection of peritubular dentine, and within these zones, rods of intratubular mineralization projecting above the surface. Stereopair, tilt angle difference = 10^{0}. BSE. Fieldwidth = 18 µm.

Figure 20. Resorption of carious dentine: field showing exposure of original intertubular matrix collagen orientation and the projection of some rods of intratubular mineralization. In some cases, resorption has removed the peritubular zone, leaving an intratubular cylinder projecting above the surface. Stereopair, tilt angle difference = 10^{0}. BSE. Fieldwidth = 18 µm.

****

resolution this could be seen to be due to the accumulation of electron dense material within the dentine tubules sometimes within pre-existing peritubular dentine zones.

In the case of very deep dentine carious lesions we could find secondary dentine formation below the cariously involved primary dentine. This tissue contained irregular numbers of irregularly oriented dentine tubules. Because of the lower number of dentine tubules, it sometimes gave the impression of having a net overall higher density than the preceding primary dentine.

Airpolishing™. The results confirmed our previous observations (Boyde, 1985) that carious dentine was eroded much more rapidly by this process than the surrounding normal tissue. Specimens of coronal dentine lesions prepared by the Airpolishing™ technique tended to show a greater extent of the dentine carious lesion than of the overlying enamel lesion (Fig. 9). This is possibly due to the fact that we deliberately selected more advanced lesions for this type of study.

Tandem scanning reflected light microscopy of carious dentine showed that the limits of carious destruction were not easily followed using the normal reflective mode. However, we have noted that under ultra violet illumination we could detect an orange auto-fluorescence of cariously involved dentine.

In the case of samples which were stained with fluorophores - including brilliant sulphaflavine, tetracycline, and alizarine - the carious dentine took up much more stain than the normal tissue and was thus clearly delineated. It was also possible to detect microorganisms in the carious dentine in the fluorescent-stained samples.

Root caries. The BSE image of longitudinal sections of normal roots shows that acellular cementum is normally more highly mineralized than dentine, even disregarding the fact that a peripheral layer of root dentine, the granular layer of Tomes, is known to be less densely mineralized than any other part of the normal dentine. The tubules of root dentine have a higher number of side branches than the coronal dentine (Mjor and Fejerskov 1979). This is also clearly illustrated in BSE images of dentine, but is particularly well shown in the TSRLM image of any longitudinally sectioned tooth.

In the root carious lesions which we have studied, the progress of the lesion was relatively shallow (Figs. 12 & 13). In other words, the extent of the lesions was greater in the plane of the root surface than downwards into the tissue. As in coronal dentine caries, the peritubular dentine was selectively removed in the carious regions. In areas where the dentine was considerably demineralized, but not totally removed, an interesting stratification of the dentine, which has also been described in demineralized tissue sections seen by light microscopy, was noted. This stratification was parallel to the incremental direction in the dentine, but was also nearly parallel to the rich side-branch network of the dentine (Fig 13). Since it is known from bacteriological studies of root caries that there is a very frequent involvement of filamentous species (e.g., Actinomyces naeslundi) it may be that the preferential splitting in this plane is enhanced by the penetration of these organisms along both the lateral branch tubules, and clefting occurring parallel to the collagenous incremental direction. The clefting may also be enhanced by shrinkage.

Mineralization-incremental features. In both root and crown dentine caries we found a high frequency of areas in which the incremental features of dentine mineralization were brought into considerable prominence (Fig. 14). Thus natural dentine caries selectively removes parts of the mineral component as a function of the time at which that mineralization had occurred. That the features we show are the original, growth-phase, incremental-mineralization growth lines (correlating with cyclic events in dentine mineralization; not matrix formation) is indicated by the fact that these lines showed the distribution of calcospherites ahead of the mineralization line, confirming that the phenomenon was solely one of mineralization, not matrix variation.

Resorption and caries.

We have two sets of observations relating to the mutual interplay of the process of dentine destruction by bacterial processes (caries) and by the normal physiological process of osteoclastic resorption.

In the first place, we note that deciduous teeth with advanced carious lesions which penetrate the pulpal cavity frequently show extensive internal resorption of the pulp chamber surface of the dentine at sites remote from the carious lesion as such, and also remote from the sites at which physiological resorption of either the external or internal surface of the deciduous tooth was occurring (Fig 15). We interpret this process as being due to the inflammation of the pulp, the internal, osteoclastic resorption of dentine being perhaps a response to cytokines produced by the inflammatory cells in the more coronal portions of the pulp.

Secondly, we have found that dentine involved

by both occlusal and interproximal carious lesions is resistant to resorption. If a tooth has at one stage been involved in an extensive caries disease process which was later "arrested", the previously affected tissue may be practically "dissected out" by the process of physiological resorption once this extends into the more coronal regions of the tooth. We can thus find shed deciduous teeth in which carious lesions project from the aboral pole of the tooth. The erupting permanent tooth may collide with the projection of (arrested) carious dentine causing a polished facet to develop on this material (Fig. 16). We are also able to demonstrate that a material may develop on the partially resorbed carious dentine which resembles a repairing, cement-like tissue. This is of interest because, in the context of periodontology, it is often assumed that microbially contaminated tissue cannot participate in a normal cementum (and hence periodontal ligament) re-attachment process.

The detail of the resorbed surface which relates to the deep, previously advancing surface, of the dentine carious lesion is particularly interesting. In such areas, we have been able to find extensive rods of peritubular dentine projecting from the resorbed surface to an extent much greater than the customary projection of peritubular dentine in the osteoclastic resorption of normal dentine (Boyde and Lester 1967) (Fig. 17). Further, many such dentine tubules contain a central rod or cylinder of material which projects even further than the cylindrical rod of peritubular dentine (Figs. 18- 20). This material would have been deposited in the dentine tubules during the time of advance of the lesion, and is frequently regarded as a normal physiological response of the odontoblasts to the advancing pathological process. It may also be due to the re-deposition of mineral dissolved by bacterial processes in the advancing dentine carious lesion. In some resorbed surfaces we have found areas where the original collagen matrix orientation pattern of the dentine is exposed by the resorption process (Figs. 18 & 20).

Discussion

The present SEM and TSRLM studies make it clear that the principal mode of progress of the carious lesion in either enamel, dentine or cement is along the axis of the major structural entities of these tissues. In enamel, the lesion progresses inwards in the general direction of the prisms, in dentine along the tubules, and in cement along the Sharpey fibres. The lateral spread of the lesion effectively relates to the area of inception caused by the thick bacterial dental plaque which creates the acidogenic and proteolytic environment for the destruction of the tissues.

In the case of enamel it is extremely doubtful if there could be anything which may be regarded as a host response to the invading carious lesion; at least, that is, until it involves the dentine. In dentine, it is debatable whether the changes peripheral to the advancing dentine lesion are properly to be regarded as host response or are an accident of the circumstances. Thus, the increased level of mineralization which can be seen deep to (but not lateral to) both occlusal and interproximal carious lesions could well be due to the liberation of the calcium and phosphate from the affected areas of the dentine. These newly formed calcium phosphates might be expected to have more acidic properties than the original carbonate-rich, apatitic mineral. More acid calcium phosphate species would require unusual biological conditions for their solubility. Thus the mineral deposited in zones peripheral to the dentine carious lesion might require more acid conditions for its dissolution, and the dissolution of the mineral component is the first step in osteoclastic resorption. This would provide one explanation for the present observation that dentine caries provides an obstruction to the normal osteoclastic resorption process. However, it must also be borne in mind that such affected dentine would have an abnormal organic matrix and may be "contaminated" with bacterial products which could specifically affect the processes of enzymatic degradation of the dentine matrix.

Carious enamel and dentine are clearly softer than sound tissues, and this fact has always been used in the exploration of the extent of, and the diagnosis of the existence of, caries in these tissues. In the present studies we have shown that the technique of Airpolishing™ - originally conceived as a process for cleaning stained plaque and calculus from teeth - can provide a means for investigating relative hardness of tissue layers in a practical fashion. We have, indeed, previously proposed that a suitable modification of the Airpolishing™ technique might be used in the excavation of carious tissue in clinical practice (Boyde 1985). We have begun microhardness studies in the SEM aimed at determining specifically whether there are increases in hardness at the advancing edge of the enamel and dentine carious lesions. We are attempting to perform these observations at a much higher resolution than has been achieved in previous microhardness sequence studies which have only been conducted at the light microscope resolution limit.

Microhardness as such is related to many factors and should not, in our opinion, be used as a measure of the degree of mineralization or of remineralization of normal and carious tissue. We have shown that it relates to the orientation of the collagen in bone and of apatite crystals in enamel (Boyde 1984b,c). It would also reflect the distribution of mineral versus pore space and organic matrix components in both tissues.

The deposition of more mineral per unit volume in (re)mineralization zones surrounding the progressing lesion is well demonstrated by the BSE imaging technique. This phenomenon would again help to explain the present observation of the selective rejection of carious dentine in the context of osteoclastic resorption.

Back-scattered electron imaging can be made quantitative. We look forward in the near future to being able to make a better quantitative description of the degree of demineralization and remineralization of enamel and dentine in both natural and artificial carious lesions, exploiting the technology which we have described (Howell and Reid 1986; Reid and Boyde 1987).

The TSRLM is useful in the study of caries because greater tissue volumes can be sampled than was heretofore possible. The TSRLM also offers the advantage in artificial caries experiments that the progress of an advancing lesion can be monitored in just the same way as has been done using polarised light studies (Silverstone 1973) and scanning x-ray microscopy (Anderson and Elliott 1985)

Acknowledgements

We gratefully acknowledge the skilled technical assistance of Elaine Maconnachie and Roy Radcliffe, and the secretarial assistance of Julie Smith. The TSRLM project has been supported by the MRC and the SERC.

References

Anderson P, Elliott JC (1985) Scanning x-ray microradiographic study of the formation of caries-like lesions in synthetic apatite aggregates. Caries Res **19**: 403-406.

Boyde A (1979) Carbonate concentration, crystal centres, core dissolution, caries, cross striations, circadian rhythms, and compositional contrast in the SEM. J Dent Res **58** Spec Issue B, Tooth Enamel III, 981-983.

Boyde A (1984a) Methodology of calcified tissue specimen preparation for SEM. In: Methods of Calcified Tissue Research (ed) Dickson GR Elsevier, Amsterdam, pp. 251-307.

Boyde A (1984b) Airpolishing effects on enamel, dentine and cement. Brit Dent J **156**: 287-291.

Boyde A (1984c) Dependence of rate of physical erosion on orientation and density in mineralized tissues. Anat Embryol **170**: 57-62.

Boyde A (1985) Anatomical considerations relating to tooth preparation. In: Resin Based Posterior Materials, (eds) Smith D, Vanherle G. 3M Co., Minneapolis, MN. 377-403.

Boyde A (1986) Applications of tandem scanning reflected light microscopy and three-dimensional imaging. Ann NY Acad Sci **483**: 428-439.

Boyde A, Jones SJ (1983) Backscattered electron imaging of dental tissues. Anat Embryol **168**: 211-226.

Boyde A, Lester KS (1967) Electron microscopy of resorbing surfaces of dental hard tissues. Z Zellforsch **83**: 538-548.

Boyde A, Switsur VR, Fearnhead RW (1961) Application of the scanning electron probe x-ray microanalyser to dental tissues. J Ultrastructure Res **5**: 201-207.

Boyde A, Switsur VR, Stewart ADG (1963) An assessment of two new physical methods applied to the study of dental tissues. Proc 9th ORCA Congress. Pergamon Press, Oxford. pp. 185-193.

Boyde A, Petran M, Hadravsky M (1983) Tandem scanning reflected light microscopy of internal features in whole bone and tooth samples. J. Microscopy **132**: 1-7.

Brannstrom M, Gola G, Nordenvall KJ, Torstenson B (1980) Invasion of microorganisms and some structural changes in incipient caries. Caries Res **14**: 276-284.

Darling AI (1958) Studies of the early lesion of enamel caries. Brit Dent J **105**: 119-135.

Fejerskov O, Josephsen K, Nyvad B (1984) Surface ultrastructure of unerupted human enamel. Caries Res **18**: 302-314.

Goldberg M, Arends J, Septier D, Jongebloed WL (1981) Microchannels in the surface zone of artificially produced caries-like enamel lesions. J Biol Buccale **9**: 297-314.

Gottlieb B, Diamond M, Applebaum E (1946) The caries problem. Oral Surgery **32**: 365-379.

Haikel Y, Frank RM, Voegel JC (1983) Scanning electron microscopy of the human enamel surface layer of incipient carious lesions. Caries Res **17**: 1-13.

Holmen L, Thylstrup A, Ogaard B, Kragh F (1985a) A scanning electron microscopic study of progressive stages of enamel caries in vivo. Caries Res **19**: 355-367.

Holmen L, Thylstrup A, Featherstone JDB, Fredebo L, Shariati M (1985b) A scanning electron microscopic study of surface changes during development of artificial caries. Caries Res **19**: 11-21.

Howell PGT, Reid SA (1986) A micro-computer based system for rapid on-line stereological analysis in the SEM. Scanning **8**: 139-144.

Johnson NW, Poole DFG, Tyler JE (1971) Factors affecting the differential dissolution of human enamel in acid and EDTA. A scanning electron microscope study. Archs Oral Biol **16**: 385-396.

Jones SJ, Boyde A (1984) Ultrastructure of dentinogenesis. In: Dentin and Dentinogenesis Vol 1 (ed) Linde A. CRC Press, Boca Raton, FL. pp. 81-134.

Jones SJ, Boyde A (1987) Dentine mineralization, demineralization and microhardness: recent studies using scanning microscopies. In: Leach SA (ed), Dentine and Dentine Reactions in the Oral Cavity. IRL Press, Oxford. in press.

Jongebloed WL, Molenaar I, Arends J (1975) Morphology and size distribution of sound and acid-treated enamel crystallites. Calcif Tiss Res **19**: 109-123.

Lester KS, Boyde A (1968a) Some preliminary observations on caries ("remineralization") crystals in enamel and dentine by surface electron microscopy. Virchow's Archiv Path Abt A Anat **344**: 196-212.

Lester KS, Boyde A (1968b) The surface morphology of some crystalline components of dentine. In: Dentine and Pulp (ed). Symons NBB. Livingstone, Edinburgh. pp.197-219.

Mjor IA, Fejerskov O (1979) The histology of the human tooth. 2nd ed. Munksgaard, Copenhagen.

Petran M, Hadravsky M, Boyde A (1985) The tandem scanning reflected light microscope. Scanning **7**: 97-108.

Reid SA, Boyde A (1987) Changes in the mineral density distribution in human bone with age: image analysis using backscattered electrons in the SEM. J Bone Mineral Res **2**: 13-22.

Shellis RP, Hallsworth AS (1987) Use of SEM in studying enamel caries. Scanning Microsc. 1(3), 1109-1123.

Silverstone LM (1973) Structure of carious enamel, including the early lesion. Oral Sci Rev **3**: 100-160.

Discussion with Reviewers

S.H. Ashrafi: Do you think that the application of TSRLM can show the progress of an advancing carious lesion as nicely as BSE SEM?
Authors: Yes.

R.P. Shellis: Do the authors identify the cross-striations as the dark bands or the light bands in the BSE images? In other words, do the cross-striations appear to be selectively dissolved or selectively spared during the formation of a carious lesion?
Authors: (Are the zebra's stripes black or white?). The narrow, dark band seen when enamel is viewed in polarised light probably also represents the narrowest region or constriction of the head of the prism, and is the region that appears less dense in BSE imaging of normal (Boyde & Jones 1983) and carious enamel. A change in the ratio of carbonate to phosphate may be implicated (Boyde 1979).

R.P. Shellis: The report of fluorescent dye penetration along prism junctions appears to conflict with the absence of change in density by BSE at the junctions at the inner border of lesions. Is this a general finding and, if so, could the authors comment on the possible reasons for it?
Authors: We have to adjust the contrast for viewing sound (rather than carious) enamel with BSE to demonstrate this change at the inner border of lesions. The TSRLM also surveys a much greater volume of tissue.

R.P. Shellis: Are the pores themselves, or the changes in refractive index at the pore/solid interfaces, responsible for the increased reflectivity of the enamel lesion seen in the TSRLM?
Authors: We presume the latter.